Metabolic profiling using combined GC–MS and LC–MS provides a systems understanding of aristolochic acid-induced nephrotoxicity in rat

By: Yan Ni, Mingming Su, Yunping Qiu, Minjun Chen, Yuming Liu, Aihua Zhao, and Wei Jia

Ni, Y., Su, M., Qiu, Y., Chen, M., Liu, Y., Jia, W. (2007) Metabolic profiling using combined GC-MS and LC-MS provides a systems understanding of aristolochic acid-induced nephrotoxicity in rat, FEBS Letters. 581(4): 707-711. doi:10.1016/j.febslet.2007.01.036

*****Note: Figures may be missing from this format of the document**

Abstract:
We present here a combined GC–MS and LC–MS metabolic profiling approach to unraveling the pathological outcomes of aristolochic acid (AA)-induced nephrotoxicity. Urine samples were analyzed by GC–MS and LC–MS in combination with pattern recognition techniques, e.g. principal component analysis (PCA), orthogonal projection to latent structure-discriminant analysis. The work indicates that AA-induced acute renal toxicity as evidenced by histopathological examinations could be characterized by systemic disturbance of metabolic network involving free fatty acids generation, energy and amino acids metabolism, and alteration in the structure of gut microbiota. Therefore, this method is potentially applicable to the toxicological study, providing a comprehensive understanding of systems response to xenobiotic intervention.
Keywords: Aristolochic acid; Metabolic profiling; Mass spectrometry; Nephrotoxicity; Pattern recognition; OPLSDA
Abbreviations: MS, mass spectrometry; GC–MS, gas chromatography–mass spectrometry; LC–MS, liquid chromatography–mass spectrometry; NMR, ^{1}H nuclear magnetic resonance; CE-MS, capillary electrophoresis-mass spectrometry; PCA, principal component analysis; OPLSDA, orthogonal projection to latent structure-discriminant analysis

Article:
1. Introduction
Aristolochic acid (AA), widely present in the botanicals, i.e. *Aristolochia*, *Bragantia* and *Asarum* species, is generally believed to cause acute renal failure (ARF), characterized by interstitial fibrosis, hyperproteinemia, severe anaemia, and uremia [1], [2], [3] and [4]. Conventional toxicological studies on AA focused merely on nephrotoxic mechanisms such as the activation or inhibition of certain enzymes related to the renal lesion [5], [6], [7], [8] and [9]. Recently, the revival of systems biology aiming to integrate all the pertinent components, e.g. genes, proteins, and metabolites, and all intricate relationship into a holistic biological network provides comprehensive thoughts in understanding and addressing systems' behavior [10] and [11].

Metabolomics/metabonomics, concomitant with genomics, metagenomics, proteomics, etc., is a newly thriving systems biology and has been highly favored in botanical science [12], environmental research [13], and toxicological study in preclinical and clinical fields [14], [15], [16] and [17]. The goal of global metabolic profiling is to monitor as many metabolites with low

molecular weight as possible in a single cell, biofluids, and tissue extracts [18]. However, none of the analytical instruments including NMR, GC–MS, LC–MS, and CE-MS has so far been able to capture the entire composition of endogenous metabolites. The use of multiple analytical methods in combination may offer a better strategy for identifying a broadened spectrum of important metabolites associated with physiological and/or pathological variations [19], [20] and [21].

It is technically challenging to integrate data from different analytical methods which measure different types of biochemical molecules generated from diverse aspects of a system, during which repercussions resulting from systematic biases, false-positive or -negative rates inherent in the high-throughput assays are to be under scrutiny [10] and [22]. To date, enormous efforts have been made to integrate a variety of data from multiple analytical platforms, which have facilitated the identification of subtle variation between two physiological states using simplified mathematical models [11], [22] and [23].

We have previously established a time-dependent changing metabonomic profile in AA-induced nephrotoxic model using HPLC-ESI-MS [24]. In this work, we repeated the previous study using GC–MS analytical technique, in which we have identified a number of important metabolites related to AA toxicity. Multivariate statistical analysis was used to process the integrated dataset generated from LC–MS and GC–MS, allowing a comprehensive understanding of mechanisms of AA-induced nephrotoxicity.

2. Materials and methods

2.1. Animal handling and sampling

The study was approved by China national legislation and local guidelines. The experimental protocols followed our previously published work [24]. Urine samples were collected at different time-points from the male Wistar rats dosed with AA or vehicle, and immediately kept at −70 °C until MS measurement.

2.2. GC–MS spectroscopy acquisition

Each 300-μL aliquot of urine sample was mixed with 300 μL of water for ethyl chloroformate (ECF)-derivatization prior to GC–MS spectral acquisition as described[25]. One microlitre of the analyte was injected into a DB-5MS capillary column coated with 5% diphenyl cross-linked 95% dimethylpolysiloxane (30 m × 250 μm i.d., 0.25 μm film thickness; Agilent J&W Scientific, Folsom, CA) performed on a hyphenated analytical technique, gas chromatography–mass spectrometry (Perkin–Elmer Inc., USA).

2.3. LC–MS spectroscopy acquisition

Details of the protocol were provided in our previously published paper [24].

2.4. Preprocessing of data

The data from the GC–MS and LC–MS analysis were converted to NetCDF format via DataBridge (Perkin–Elmer Inc.) and Agilent LC/MSD ChemStation (Rev.B.01.03, Agilent Tech., USA), respectively. Each file was extracted subsequently using our custom scripts in the MATLAB 7.0 (The MathWorks, Inc., USA), where baseline correction, and peak resolving and alignment were carried out. The output data were organized in the form of arbitrary peak index

(retention time–*m*/*z* pair), sample names (observations), and peak intensity information (variables).

Directly concatenating the matrices of processed-MS data is sub-optimal as this may result in a matrix with an unfavorable samples-to-variables ratio [22]. It is necessary to use properly reduced matrix to conduct multivariate statistical analysis. Notably, GC–MS data inherently contain apparent variability and complexity such as multiple fragments from a single compound. A simple strategy was to combine these fragments with the same retention time into a single compound. The binning procedure should be manually confirmed by comparing the major ion fragments of a compound detected with those from commercially available and in-house libraries in order to minimize the prejudice to confounding peaks. Using previously established GC–MS analysis protocol, we detected about 200–250 different urine metabolites, with 87 of them identified by means of the library or verified via authentic standards. Lacking the effective peak resolving method for LC–MS data, we used an optimized voltage, which is kept stable and constant throughout the experiment, to obtain a number of the corresponding molecular ions $[M+H^+]$ deriving from endogenous metabolites. Ultimately, an integrated matrix was obtained for subsequent multivariate statistical analysis by merging the two sets of data.

Since MS-data were obtained from different analytical instruments and urine volume varied over subjects, block normalization to the total sum of the chromatogram was conducted on GC–MS and LC–MS data, respectively. The internal standard for on-line supervising inter-batch reproducibility and for automated peak matching algorithm of retention time was removed prior to the normalization. Mean-centering was performed columnwise to remove the offsets and autoscaling (scaled to unit variance) to put all the measured metabolites on an equal level. That is, metabolites present at low concentrations are of equal importance with those present at high concentrations.

2.5. Multivariate statistical analysis

GC–MS and LC–MS data of urine samples from the two groups (AA-induced nephrotoxicity group versus the healthy control) at the 7th day postdose were analyzed by principal component analysis (PCA) to envisage the perturbation of the metabolic network of the AA-treated animals. Orthogonal projection to latent structure-discriminant analysis (OPLSDA) was carried out on the integrated MS data allowing the identification of differential metabolites in the urine. In the OPLSDA algorithm, the variation in **X** (the combined MS data) is decomposed into three parts: the first being the variation in **X** related to **Y** (the class variable, e.g., 0/1), and the last two containing the specific systemic variation in **X** and residual, respectively. This leads to a model with a minimal number of predictive components defined by the number of degrees of freedom ($k - 1$ dimensions) between group variances (k classes). Therefore, the interpretation of differential metabolites in the two groups is straightforward using one loading alone. To validate the model against over-fitting, the prediction accuracy (cross-validation parameter) $\mathbf{Q}^2_{\hat{Y}}$ was computed. Details regarding OPLSDA algorithm are available in other publications [26].

3. Results

3.1. PCA of integrated MS matrix

The scores plot (PC1 versus PC2) derived from the integrated MS-data (Fig. 1) depicted two distinct clustering without any overlap between the groups (AA-treated group and the healthy

control). The separation of the two groups occurred in the PC1, and the cluster appeared to be tighter in the healthy control group as compared to the AA-dosed group. These findings were in good agreement with LC–MS-based metabolic profiles as well as the histopathological examination [24].

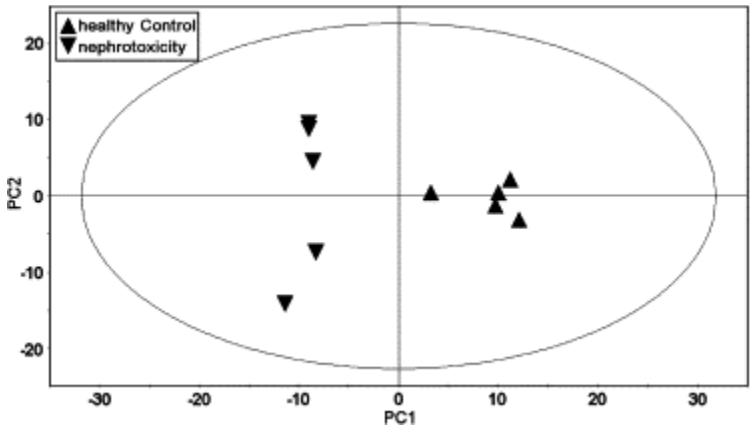

Fig. 1. PCA scores plot (PCI versus PC2) derived from the integrated MS data of urine samples obtained from AA-induced nephrotoxicity rats (▼) and the healthy control (▲). Hotelling T2 ellipse = 95% confidence limit.

3.2. Investigation of the differential metabolites by OPLSDA

OPLSDA model was generated with one predictive component, and one orthogonal component to discriminate the two group rats. R^2X and R^2Y represented the fraction of the variation of all the *X* variables (the combined MS data) and the "dummy" *Y* variables (0/1) by the model, respectively. The R^2Y values in this work (approximately 1.0) suggested a satisfactory model (Fig. 2a). The prediction accuracy ($Q^2Y > 0.75$) obtained through a typical 7-fold cross-validation further guaranteed the models (Fig. 2a). Additionally, the distance to model is calculated for each sample using the integrated MS data (a critical value of 99.5% for outliers marked as a dashed line) in case of spurious effects of outlying samples (Fig. 2b). However, no outlying data point was observed at this threshold, meaning that any metabolite of interest mirrored the general effects after exposure to AA. The correlation coefficients ($r > 0.70$ was considered as having good discriminant ability) resulting from OPLSDA of the integrated MS data were summarized in Table 1, where the metabolites were designated according to the corresponding GC–MS and LC–MS analyses. The reduced urinary excretion levels of citrate, aconinate, isocitrate, succinate, *m*-hydroxyphenylpropionate, caprylic acid, valeric acid, arachidonic acid, methionine, and elevated levels of serine, *p*-cresol, *p*-hydroxyphenylacetate, cystine, cysteine, and homocysteine were detected in the AA-dosed rats as compared to the healthy controls. These metabolites were identified by authentic standards available (Sigma–Aldrich, USA) and the commercial compound libraries: NIST, Wiley in Turbomass 4.1.1 software (Perkin–Elmer Inc.). No overlap in analytical outcomes was observed between the two methods probably due to the difference between the GC–MS and LC–MS techniques.

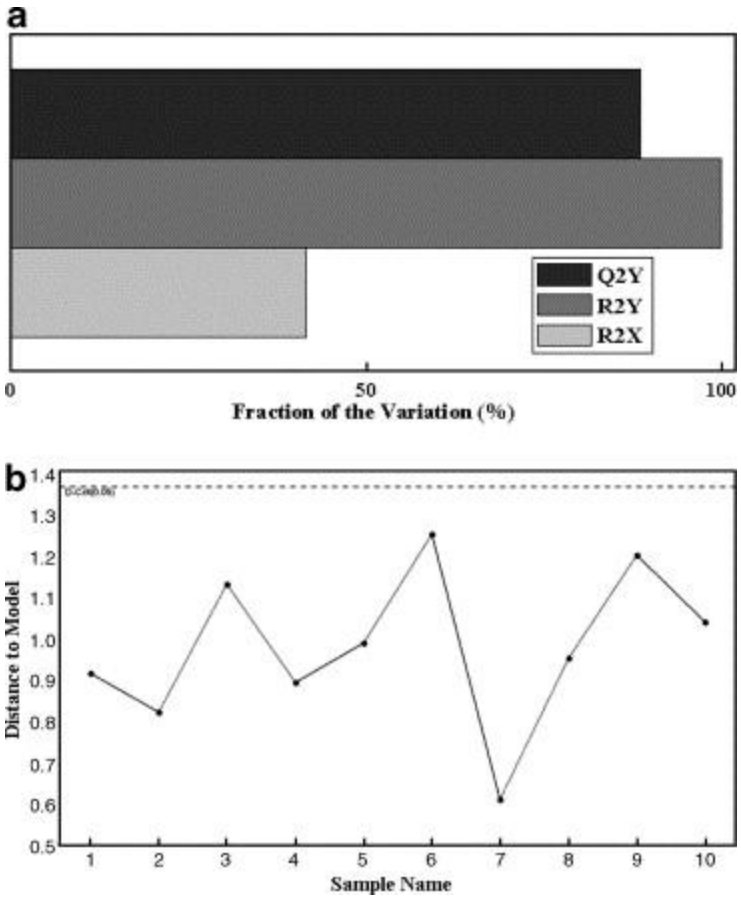

Fig. 2. (a) OPLSDA model summary of the combined MS dataset. For more explanation of the R^2X, R^2Y, and Q^2Y values, see the text. (b) The distance to model plot. (•, sample values).

Table 1.
A list of most profound metabolites relevant to the AA-induced nephrotoxicity

Metabolites (GC–MS)	**Correlation coefficients[a]**	**Metabolites (LC–MS)**	**Correlation coefficients[a]**
Citrate	−0.83 (↓)	Caprylic acid	−0.84 (↓)
Aconitate	−0.76 (↓)	Valeric acid	−0.92 (↓)
Isocitrate	−0.91 (↓)	Arachidonic acid	−0.79 (↓)
Succinate	−0.79 (↓)	Methionine	−0.81 (↓)
m-Hydroxyphenylpropionate	−0.74 (↓)	Serine	0.92 (↑)
p-Cresol	0.84 (↑)	Homocysteine	0.78 (↑)
p-Hydroxyphenylacetate	0.79 (↑)		

Metabolites (GC–MS)	Correlation coefficients[a]	Metabolites (LC–MS)	Correlation coefficients[a]
Cystine	0.81 (↑)		
Cysteine	0.92 (↑)		

[a] The correlation coefficients shown are based on the OPLSDA of the integrated MS dataset, positive value indicates an increase of the metabolites in the AA-dosed group (denoted by an up-arrow), whereas negative value represents a decreased level of the metabolites in this group.

4. Discussion

In this study, we have verified the previous research results using a different analytical method. Based on the integrated MS matrix, we have adopted OPLSDA to identify the perturbed metabolic pathways relating to AA-induced nephrotoxicity. The work suggested that the application of different analytical methods may capture different sets of endogenous metabolites with unique biological significance, and that integration of dataset from multi-analytical platforms is technically feasible and of great significance for a comprehensive understanding of systemic perturbation.

Metabolic disorder of amino acids, homocysteine and serine in particular, is commonly used as the criteria for diagnosis of kidney morbidity [5], [6], [7], [8] and [9]. In this study, such disturbed amino acids as cystine, cysteine, homocysteine, methionine, and serine identified in the urine probably reflected the impaired renal tubule and subsequent cellular interstitial fibrosis due predominately to the direct cytotoxic effects of AA on kidney [27]. In addition, the significant variations of homocysteine and methionine were detected by LC–MS analysis, whereas changes in cystine and cysteine concentration were observed by GC–MS analysis. Combining the results obtained from two analytical methods together, a disturbed metabolic pathway emerged (Fig. 3a) [28], benefiting from the use of two complementary methods.

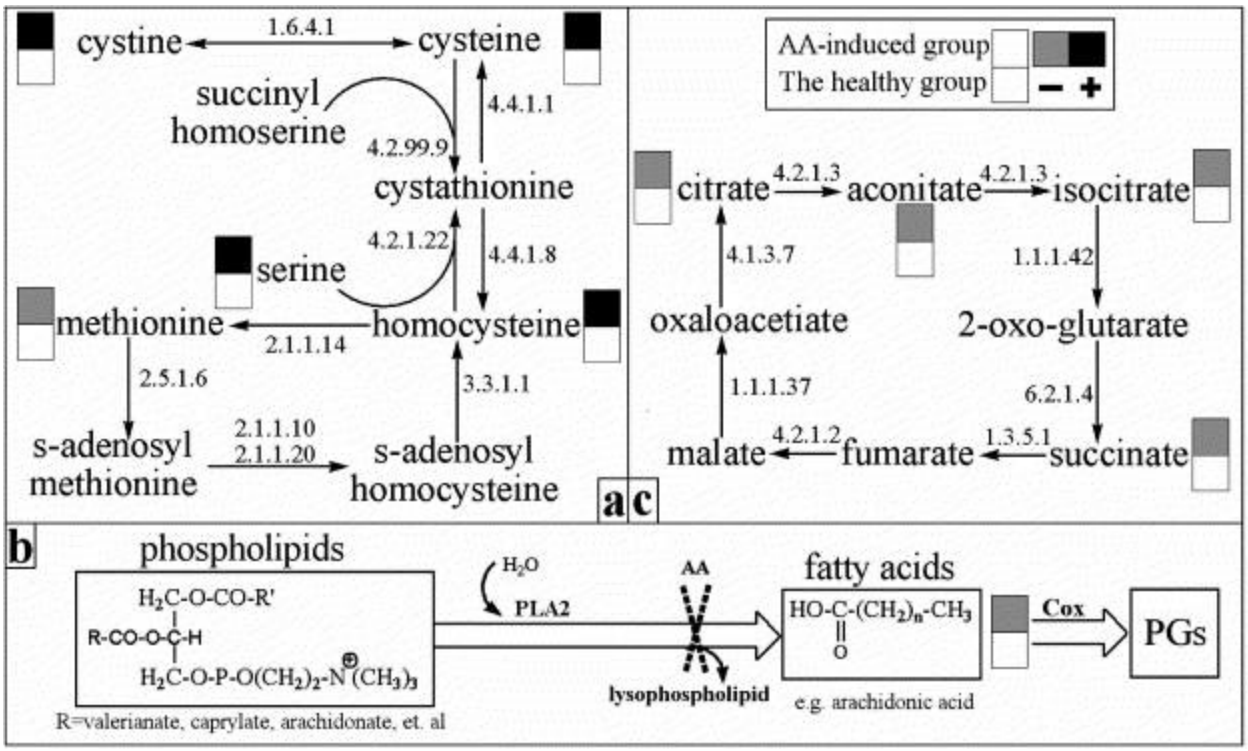

Fig. 3. The perturbed metabolic pathways in response to AA exposure: (a) AA-induced metabolic disorder of amino acids; (b) AA perturbed TCA cycle; (c) PLA2-related mechanisms of AA-induced nephrotoxicity. Dark square denotes an elevated concentration of metabolites present in the urine from rats exposed to AA, whereas gray square means a reduced level of metabolites in this group as compared to the healthy.

The negative OPLSDA correlation coefficients of the fatty acids such as caprylic acid, valeric acid and arachidonic acid, indicated the declined levels of these metabolites in the AA-dosed group as compared to the healthy control. Arachidonic acid, an intermediate in the production of prostaglandins (PGs), is produced during the process of phospholipids hydrolyzation by means of phospholipase A2 (PLA2) into lecithin and phosphatidylinostitol. Phospholipase A2 (PLA2) is greatly inhibited by AA, leading to a reduced level of arachidonic acid (Fig. 3b) [28], [29], [30], [31] and [32]. The down-regulated production of arachidonic acid may negatively impact the production of PGs which play important roles in renal functions, e.g. attenuating renal vasodilatation, regulating renal circulation, and affecting renal sodium excretion and water reabsorption, ultimately leading to kidney lesion [33]. It is therefore assumed that depletion of arachidonic acid may be one of the fundamental causes of acute renal failure induced by AA.

GC–MS analytical method was able to identify the significant variations of phenyl-containing compounds such as *p*-cresol, *p*-hydroxyphenylacetate, and *m*-hydroxyphenylpropionate. These compounds are manipulated mainly by gut microbiota in the living systems through fermentation of dietary polyphenols and aromatic amino acids [34]. The variations in phenyl-containing metabolites suggested that the gut microbiota was greatly restructured by the AA intervention. The principal metabolites of AA are aristolactam I, aristolactam Ia, and aristolactam II that are produced through classical bacterial nitroreductase, and these aristolactams are the precursors of AA–DNA adducts responsible for triggering or accelerating a fibrotic process [35], [36], [37]

and [38]. In this context, the significant disorders of symbiotic bacteria may be indicative of AA-induced acute kidney lesion.

It has been well documented that citrate, aconite, iso-citrate and succinate are the crucial substances of tricarboxylic acids (TCA) cycle (Fig. 3c) [28], which is the main pathway of glucose degradation and is primary energy supplier for universal organisms. Following the nephrotoxicity induced by AA, these compounds were significantly decreased when compared with the healthy control animals, suggesting that AA may inhibit the activity of these compounds, ultimately repressing energy metabolism [39] and [40]. This finding was consistent with the experimental observations on AA-treated rats with much reduced daily activity and a tendency to press close together.

The combined use of multiple analytical instruments, such as GC–MS and LC–MS, takes advantage of complementary outcomes and therefore, provides an improved analytical means for explaining the biological variation in the living systems. Our study using the combined MS-based metabolic profiling technique has revealed that AA led to direct cytotoxic effect and enzyme inhibition, and to the significant alteration of gut-motivated metabolites and energy metabolism, ultimately leading to a disruption of the kidney-related metabolic regulatory network and renal function.

Acknowledgement

This work was supported by Shanghai Leading Academic Discipline Project, Project No. T0301.

References

[1] C. Isnard Bagnis, G. Deray, A. Baumelou, M. Le Quintrec and J.L. Vanherweghem, Herbs and the kidney, *Am. J. Kidney Dis.* **44** (2004), pp. 1–11.

[2] U. Mengs, Acute toxicity of aristolochic acid in rodents, *Arch. Toxicol.* **59** (1987), pp. 328–331.

[3] U. Mengs and C.D. Stotzem, Renal toxicity of aristolochic acid in rats as an example of nephrotoxicity testing in routine toxicology, *Arch. Toxicol.* **67** (1993), pp. 307–311.

[4] J.L. Vanherweghem *et al.*, Rapidly progressive interstitial renal fibrosis in young women: association with slimming regimen including Chinese herbs, *Lancet* **341** (1993), pp. 387–391.

[5] Y.E. Taes, J.R. Delanghe, A.S. De Vriese, R. Rombaut, J. Van Camp and N.H. Lameire, Creatine supplementation decreases homocysteine in an animal model of uremia, *Kidney Int.* **64** (2003), pp. 1331–1337.

[6] B.S. Vishwanath, R.M. Kini and T.V. Gowda, Characterization of three edema-inducing phospholipase A2 enzymes from habu (*Trimeresurus flavoviridis*) venom and their interaction with the alkaloid aristolochic acid, *Toxicon* **25** (1987), pp. 501–515.

[7] R.E. Williams and E.A. Lock, Sodium benzoate attenuates d-serine induced nephrotoxicity in the rat, *Toxicology* **207** (2005), pp. 35–48.

[8] L. Yang, X. Li and H. Wang, Possible mechanisms explaining the tendency towards interstitial fibrosis in aristolochic acid-induced acute tubular necrosis, *Nephrol. Dial. Transplant* (2006).

[9] C. Zoccali, Biomarkers in chronic kidney disease: utility and issues towards better understanding, *Curr. Opin. Nephrol. Hypertens.* **14** (2005), pp. 532–537.

[10] L. Hood and R.M. Perlmutter, The impact of systems approaches on biological problems in drug discovery, *Nat. Biotechnol.* **22** (2004), pp. 1215–1217.
[11] D. Hwang *et al.*, A data integration methodology for systems biology: experimental verification, *Proc. Natl. Acad. Sci. USA* **102** (2005), pp. 17302–17307.
[12] O. Fiehn, J. Kopka, P. Dormann, T. Altmann, R.N. Trethewey and L. Willmitzer, Metabolite profiling for plant functional genomics, *Nat. Biotechnol.* **18** (2000), pp. 1157–1161.
[13] M.R. Viant, E.S. Rosenblum and R.S. Tieerdema, NMR-based metabolomics: a powerful approach for characterizing the effects of environmental stressors on organism health, *Environ. Sci. Technol.* **37** (2003), pp. 4982–4989.
[14] M.E. Bollard, A.J. Murray, K. Clarke, J.K. Nicholson and J.L. Griffin, A study of metabolic compartmentation in the rat heart and cardiac mitochondria using high-resolution magic angle spinning 1H NMR spectroscopy, *FEBS Lett.* **553** (2003), pp. 73–78.
[15] T.A. Clayton *et al.*, Pharmaco-metabonomic phenotyping and personalized drug treatment, *Nature* **440** (2006), pp. 1073–1077.
[16] R.J. Mortishire-Smith, G.L. Skiles, J.W. Lawrence, S. Spence, A.W. Nicholls, B.A. Johnson and J.K. Nicholson, Use of metabonomics to identify impaired fatty acid metabolism as the mechanism of a drug-induced toxicity, *Chem. Res. Toxicol.* **17** (2004), pp. 165–173.
[17] A.W. Nicholls, R.J. Mortishire-Smith and J.K. Nicholson, NMR spectroscopic-based metabonomic studies of urinary metabolite variation in acclimatizing germ-free rats, *Chem. Res. Toxicol.* **16** (2003), pp. 1395–1404.
[18] J.K. Nicholson, J.C. Lindon and E. Holmes, „Metabonomics': understanding the metabolic responses of living systems to pathophysiological stimuli via multivariate statistical analysis of biological NMR spectroscopic data, *Xenobiotica* **29** (1999), pp. 1181–1189.
[19] R. Williams, E.M. Lenz, A.J. Wilson, J. Granger, I.D. Wilson, H. Major, C. Stumpf and R. Plumb, A multi-analytical platform approach to the metabonomic analysis of plasma from normal and zucker (fa/fa) obese rats, *Mol. Biosyst.* **2** (2006), pp. 174–183.
[20] R.E. Williams, E.M. Lenz, J.A. Evans, I.D. Wilson, J.H. Granger, R.S. Plumb and C.L. Stumpf, A combined (1)H NMR and HPLC-MS-based metabonomic study of urine from obese (fa/fa) Zucker and normal Wistar-derived rats, *J. Pharm. Biomed. Anal.* **38** (2005), pp. 465–471.
[21] R.E. Williams, E.M. Lenz, J.S. Lowden, M. Rantalainen and I.D. Wilson, The metabonomics of aging and development in the rat: an investigation into the effect of age on the profile of endogenous metabolites in the urine of male rats using 1H NMR and HPLC-TOF MS, *Mol. Biosyst.* **1** (2005), pp. 166–175.
[22] A.K. Smilde, M.J. van der Werf, S. Bijlsma, B.J. van der Werff-van der Vat and R.H. Jellema, Fusion of mass spectrometry-based metabolomics data, *Anal. Chem.* **77** (2005), pp. 6729–6736.
[23] M. Rantalainen *et al.*, Statistically integrated metabonomic–proteomic studies on a human prostate cancer xenograft model in mice, *J. Proteome Res.* **5** (2006), pp. 2642–2655.
[24] M. Chen *et al.*, Metabonomic study of aristolochic acid-induced nephrotoxicity in rats, *J. Proteome Res.* **5** (2006), pp. 995–1002.
[25] Y. Qiu, M. Su, Y. Liu, M. Chen, J. Gu, J. Zhang and W. Jia, Application of ethyl chloroformate derivatization for gas chromatography–mass spectrometry based metabonomic profiling, *Anal. Chim. Acta.* **2** (2007), pp. 277–283.
[26] O. Cloarec *et al.*, Statistical total correlation spectroscopy: an exploratory approach for latent biomarker identification from metabolic 1H NMR data sets, *Anal. Chem.* **77** (2005), pp. 1282–1289.

[27] P. Balachandran, F. Wei, R.C. Lin, IA. Khan and D.S. Pasco, Structure activity relationships of aristolochic acid analogues: toxicity in cultured renal epithelial cells, *Kidney Int.* **67** (2005), pp. 1797–1805.
[28] <http://www.genome.jp/kegg/pathwav.html>.
[29] O. Fourcade *et al.*, Secretory phospholipase A2 generates the novel lipid mediator lysophosphatidic acid in membrane microvesicles shed from activated cells, *Cell* **80** (1995), pp. 919–927.
[30] J.J. Moreno, Effect of aristolochic acid on arachidonic acid cascade and in vivo models of inflammation, *Immunopharmacology* **26** (1993), pp. 1–9.
[31] M.D. Rosenthal, B.S. Vishwanath and R.C. Franson, Effects of aristolochic acid on phospholipase A2 activity and arachidonate metabolism of human neutrophils, *Biochim. Biophys. Acta* **1001** (1989), pp. 1–8.
[32] R.T. Worrell, H.F. Bao, D.D. Denson and D.C. Eaton, Contrasting effects of cPLA2 on epithelial Na^+ transport, *Am. J. Physiol. Cell Physiol.* **281** (2001), pp. C147–C156.
[33] G. Giovanni and P. Giovanni, Do non-steroidal anti-inflammatory drugs and COX-2 selective inhibitors have different renal effects?, *J. Nephrol.* **15** (2002), pp. 480–488.
[34] Y. Wang, E. Holmes, J.K. Nicholson, O. Cloarec, J. Chollet, M. Tanner, B.H. Singer and J. Utzinger, Metabonomic investigations in mice infected with Schistosoma mansoni: an approach for biomarker identification, *Proc. Natl. Acad. Sci. USA* **101** (2004), pp. 12676–12681.
[35] J.P. Cosyns, J.P. Dehoux, Y. Guiot, R.M. Goebbels, A. Robert, A.M. Bernard and C. van Ypersele de Strihou, Chronic aristolochic acid toxicity in rabbits: a model of Chinese herbs nephropathy?, *Kidney Int.* **59** (2001), pp. 2164–2173.
[36] G. Gillerot, E. GofFin, P. Moulin, V.M. Arlt, D.H. Phillips, J.P. Cosyns and O. Devuyst, Aristolochic acid nephropathy and the peritoneum: functional, structural, and molecular studies, *Kidney Int.* **64** (2003), pp. 1883–1892.
[37] C. Lebeau, V.M. Arlt, H.H. Schmeiser, A. Boom, P.J. Verroust, O. Devuyst and R. Beauwens, Aristolochic acid impedes endocytosis and induces DNA adducts in proximal tubule cells, *Kidney Int.* **60** (2001), pp. 1332–1342.
[38] W. Li, D.F. Choy, M.S. Lam, T. Morgan, M.E. Sullivan and J.M. Post, Use of cultured cells of kidney origin to assess specific cytotoxic effects of nephrotoxins, *Toxicol. In Vitro* **17** (2003), pp. 107–113.
[39] V.M. Buckalew Jr., Nephrolithiasis in renal tubular acidosis, *J. Urol.* **141** (1989), pp. 731–737.
[40] K.P. Gartland, C.R. Beddell, J.C. Lindon and J.K. Nicholson, Application of pattern recognition methods to the analysis and classification of toxicological data derived from proton nuclear magnetic resonance spectroscopy of urine, *Mol. Pharmacol.* **39** (1991), pp. 629–642.